Horizon 2020
European Union funding
for Research & Innovation

Horizon 2020 Grant Agreement Number 734798

indoor small-cell Networks with 3D MIMO Array Antennas (is3DMIMO)

D3.2

Report on fundamental performance limits of densely deployed small-cell APs with optimized 3D MIMO configurations

Authors(s)	Hui Zheng, Jiliang Zhang and Haonan Hu
Author(s) Affiliation	University of Sheffield, UK; Lanzhou University, Chongqing University of Posts and Telecommunications, China
Editor(s):	Xiaoli Chu and Jie Zhang
Status-Version:	Final-version
Project Number:	734798
Project Title:	indoor small-cell Networks with 3D MIMO Array Antennas (is3DMIMO)
Project Acronym:	is3DMIMO
Work Package Number	3

Abstract

In the effort to satisfy the exponential growth in wireless traffic, the three-dimensional (3D) multiple-input multiple-output (MIMO) has been considered as a key enabling technology to offer a high beamforming capability and to reduce the inter-cell interference in densely deployed small-cell (SC) networks. One open problem that the academia and industry need to investigate is how a dense SC network performs with 3D MIMO. In order to analyse the performance of dense SC networks equipped with 3D MIMO, the first step is to accurately analyse the performance of 3D dense SC networks by considering the particular features of network densification, e.g. very short link lengths. As the majority (almost 80%) of wirelss communication occur in indoor environments, this deliverable mainly focuses on the indoor 3D dense SC networks. Previous works on the performance analysis for indoor SC networks were largely based on simplified path loss models, which do not distinguish between line-of-sight (LOS) and non-line-of-sight (NLOS) transmissions. However, with the network becoming denser, both the desired signal transmission links and interference links are likely to become LOS due to the shorter distances between users and base stations (BSs). This deliverable will firstly investigate a practical path loss model including both LOS and NLOS propagations. Then, a novel and tractable LOS probability model in indoor 3D scenarios will be proposed. Finally, a mathematically tractable approach will be developed to analyse the performance of indoor 3D dense SC networks based on the proposed path loss model and LOS probability model. We obtain the analytical expressions for three performance metrics, including the coverage probability, spectral efficiency (SE) and area spectral efficiency (ASE). The analytical results are verified by Monte Carlo simulations. Based on the numerical results, we discuss the impact of BS density and LOS probability on the aforementioned network performance metrics, and provide guidelines for designing the indoor dense 3D SC networks.

Keywords: 3D dense small-cell (SC) networks, indoor environment, line-of-sight (LOS), non-line-of-sight (NLOS)

Table of Contents

Index of Figures

1 Introduction

In recent years, cellular networks are facing increasing demand and requirements in terms of the higher throughput, lower latency, and higher reliability under higher connectivity density and mobility [1]. Herein, for indoor hotspots, it is urgent to meet the higher throughput requirement, since wireless applications with the high demand of data transmission rates are still growing, such as ultra high resolution live videos and virtual reality. In this context, dense small cell (SC) networks have been considered as an effective solution to improve the throughput for indoor communication networks [2]. In dense indoor SC networks, the base stations (BSs) can be densely deployed at various locations, e.g., ceilings, floors and internal walls. The deployment of BSs apparently presents a three-dimensional (3D) layout [3]. As the majority (almost 80%) of wireless communication occur in indoor environments, the indoor scenario is a significant part of 3D SC network.

For performance analysis of SC networks, traditional approaches were based on the simplistic path loss models that did not differentiate between ling-of-sight (LOS) and non-line-of-sight (NLOS) propagations [4–6]. This results in inaccurate analysis of SC networks. The work [4] showed that, when the BS density is large enough, performance metrics such as coverage probability and spectral efficiency (SE) are not sensitive to the BS density, while the area spectral efficiency (ASE) is proportional to the BS density. However, these conclusions do no always hold when the path loss model is comprised of LOS and NLOS transmissions [7–10]. In [7], the authors explored the effects of the multi-slope path loss model, using different path loss exponents according to various distance ranges, on the dense SC networks. In [8–10], the authors investigated the piece-wise expressions of path loss incorporating both LOS and NLOS transmissions. On this basis, the performance metrics, i.e. the coverage probability and the ASE, were derived as functions of the BS density. Moreover, numerical results therein showed that the coverage probability increases with the BS density and then decreases after the BS density becomes larger than threshold. The ASE is non-linear with the BS density, which is different from the conclusion in [4–6].

We note that all the above works focused on outdoor SC networks in two-dimensional (2D) scenarios. There are very limited reported research on indoor 3D SC networks while considering LOS and NLOS transmissions. Motivated by the above limitations in the current literature, this deliverable will propose a tractable approach to investigate the performance of indoor 3D SC networks while differentiating LOS and NLOS propagations. Firstly, a multi-slope piece-wise path loss model will be employed to analyse the network performance. Next, a novel LOS probability function for indoor 3D scenarios

will be proposed. Based on the multi-slope piece-wise path loss model and the LOS probability function, the analytical expressions of three performance metrics, i.e., coverage probability, spectral efficiency (SE), and area spectral efficiency (ASE), will be derived for both a general path loss model and a special path loss model respectively based on the analysis of stochastic geometry. Note that, the content of this deliverable was partly presented in the paper [11].

The remainder of this deliverable is organized as follows. The system model is introduced in Section 2. The analytical expressions of performance metrics are derived in Section 3. The analytical results are validated by simulation results in Section 4. In the end, this deliverable is concluded in Section 5.

2 System Model

This section introduces the system model for analysing the performance of indoor 3D dense SC networks. The deliverable mainly focuses on the downlink propagations for indoor users, which are assumed to be only served by indoor BSs. The details are presented as follows.

2.1 3D Dense Small-Cell Network Model

The positions of BSs and users are modelled by two independent 3D homogeneous poisson point processes (PPPs) Φ_B with density λ_B and Φ_U with density λ_U, respectively. Moreover, assume λ_U is much larger than λ_B such that each base station will have at least one associated user in its coverage and be activated. Each BS transmits with the identical power P_t. Fig. 1 presents a 3D SC network in a 3D building consisting of many small cuboid, in which the BSs and users are randomly located. For simplicity, Fig. 1 only gives a part of the 3D building.

2.2 Path Loss Model

In order to practically describe the LOS and NLOS transmissions, the piece-wise path loss model considering the practical LOS and NLOS transmissions, is adopted with respect to

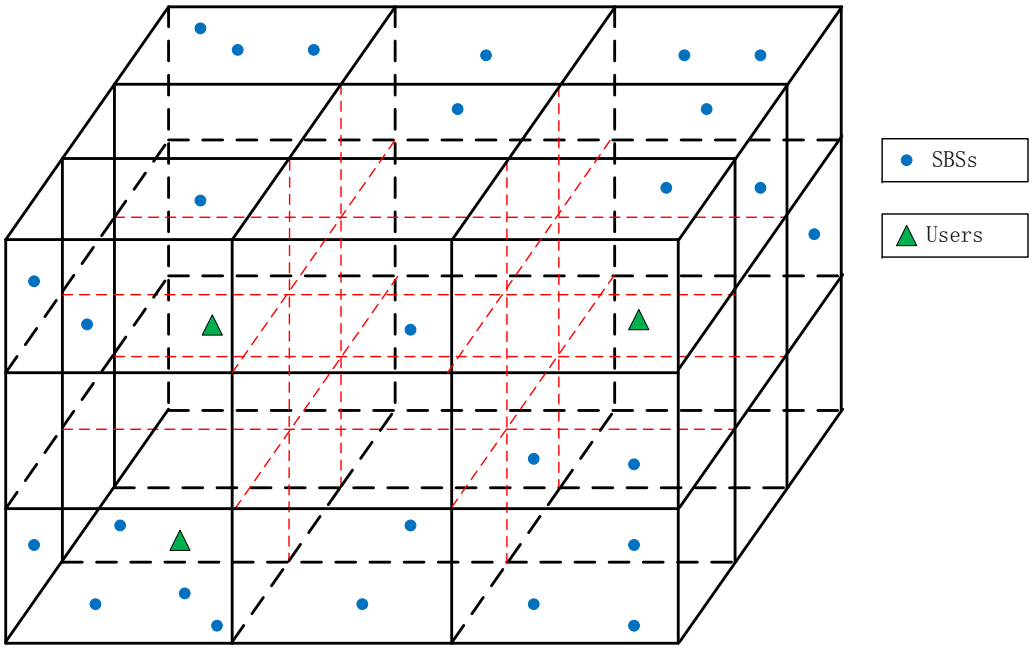

Figure 1: The typical indoor 3D network model

the link distance r between the typical user and the considered BS, which is presented as

$$\omega(r) = \begin{cases} \omega_1(r) = \begin{cases} \omega_1^{\mathrm{L}}(r), & \text{with probability } \mathrm{Pr}_1^{\mathrm{L}}(r) \\ \omega_1^{\mathrm{NL}}(r), & \text{with probability } \mathrm{Pr}_1^{\mathrm{NL}}(r) \end{cases}, & \text{when } 0 \le r \le d_1 \\ \omega_2(r) = \begin{cases} \omega_2^{\mathrm{L}}(r), & \text{with probability } \mathrm{Pr}_2^{\mathrm{L}}(r) \\ \omega_2^{\mathrm{NL}}(r), & \text{with probability } \mathrm{Pr}_2^{\mathrm{NL}}(r) \end{cases}, & \text{when } d_1 < r \le d_2 \\ \vdots & \vdots \\ \omega_N(r) = \begin{cases} \omega_N^{\mathrm{L}}(r), & \text{with probability } \mathrm{Pr}_N^{\mathrm{L}}(r) \\ \omega_N^{\mathrm{NL}}(r), & \text{with probability } \mathrm{Pr}_N^{\mathrm{NL}}(r) \end{cases}, & \text{when } r > d_{N-1} \end{cases} \tag{1}$$

where the function of path loss $\omega(r)$ is divided into N pieces, represented by $\omega_n(r)$, $n \in \{1, 2, 3, \cdots, N\}$. In addition, the variables $\omega_n^{\mathrm{L}}(r)$ and $\omega_n^{\mathrm{NL}}(r)$ denote the n-th piece path loss function for LOS and NLOS propagations, respectively. Similarly, the variables $\mathrm{Pr}_n^{\mathrm{L}}(r)$ and $\mathrm{Pr}_n^{\mathrm{NL}}(r)$ represent the n-th segment of the LOS and NLOS probability function, respectively. Note that, for each piece n, $\mathrm{Pr}_n^{\mathrm{L}}(r) + \mathrm{Pr}_n^{\mathrm{NL}}(r) = 1$.

Moreover, for each piece $\omega_n(r)$, it is modeled as

$$\omega_n(r) = \begin{cases} \omega_n^{\mathrm{L}}(r) = K_n^{\mathrm{L}} r^{-\alpha_n^{\mathrm{L}}}, & \text{for LOS transmission} \\ \omega_n^{\mathrm{NL}}(r) = K_n^{\mathrm{NL}} r^{-\alpha_n^{\mathrm{NL}}}, & \text{for NLOS transmission} \end{cases} \tag{2}$$

where the path loss exponents are denoted by α_n^{L} and α_n^{NL} for the LOS and NLOS path,

respectively. The variables K_n^{L} and K_n^{NL} are the reference path loss at a unit distance (1m), for the LOS and NLOS path, respectively. In general, the value of α_n^{L} is smaller than that of α_n^{NL}, since the negative effects of the obstacles (e.g., buildings, walls and corridors) will cause a higher attenuation of NLOS transmissions as compared with the LOS cases. In reality, the above four important path loss parameters are constants and can be obtained from channel measurement campaigns.

As shown in equation (1), $\mathrm{Pr}_n^{\mathrm{L}}(r)$ is the n-th piece LOS probability function, which monotonically decreases with distance r. Therefore, it can also be modeled as a piece-wise function, which is given by

$$\mathrm{Pr}^{\mathrm{L}}(r) = \begin{cases} \mathrm{Pr}_1^{\mathrm{L}}(r), & \text{when } 0 \leq r \leq d_1 \\ \mathrm{Pr}_2^{\mathrm{L}}(r), & \text{when } d_1 < r \leq d_2 \\ \vdots & \vdots \\ \mathrm{Pr}_N^{\mathrm{L}}(r), & \text{when } r > d_{N-1} \end{cases} \tag{3}$$

Combining equations (1), (2) and (3), the proposed path loss model can be obtained completely. It is line with the path loss model adopted by the 3GPP standards [12]. Furthermore, the path loss model with a single slope (i.e., $\omega(r) = Kr^{-\alpha}$), which has been widely used in the current communication literature, can be considered as a special case of (1) with the following parameters: $N = 1, K_1^{\mathrm{L}} = K_1^{\mathrm{NL}} = K, \alpha_1^{\mathrm{L}} = \alpha_1^{\mathrm{NL}} = \alpha, \mathrm{Pr}^{\mathrm{L}}(r) = 1, \mathrm{Pr}^{\mathrm{NL}}(r) = 0$. Remarkably, our developed path loss model will be more complex to use in network performance analysis than the simplistic ones. But its results are more practical and accurate, especially in the denser SC networks, since the transmissions are more likely to be LOS with the link distance being shorter.

Finally, in this deliverable, the user association strategy (UAS) is the smallest path loss based UAS, which is more practical than the shorted distance based UAS. Assume both the LOS and NLOS transmissions experience Rayleigh fading, which (the power gain) can be modeled as an exponential distribution with a unit mean, $h \sim \exp(1)$.

2.3 The Line-of-Sight Probability Model in Indoor 3D Scenarios

In order to obtain an exact LOS probability function, a possible pathway is to randomly generate a huge number of propagation links within an indoor 3D scenario, and then statistically count the proportion of LOS links among all generated links. Inspired by the work [13] that provides an approach to derive the LOS probability function in indoor 2D scenarios, this deliverable extends the modelling LOS probability to the indoor 3D environments.

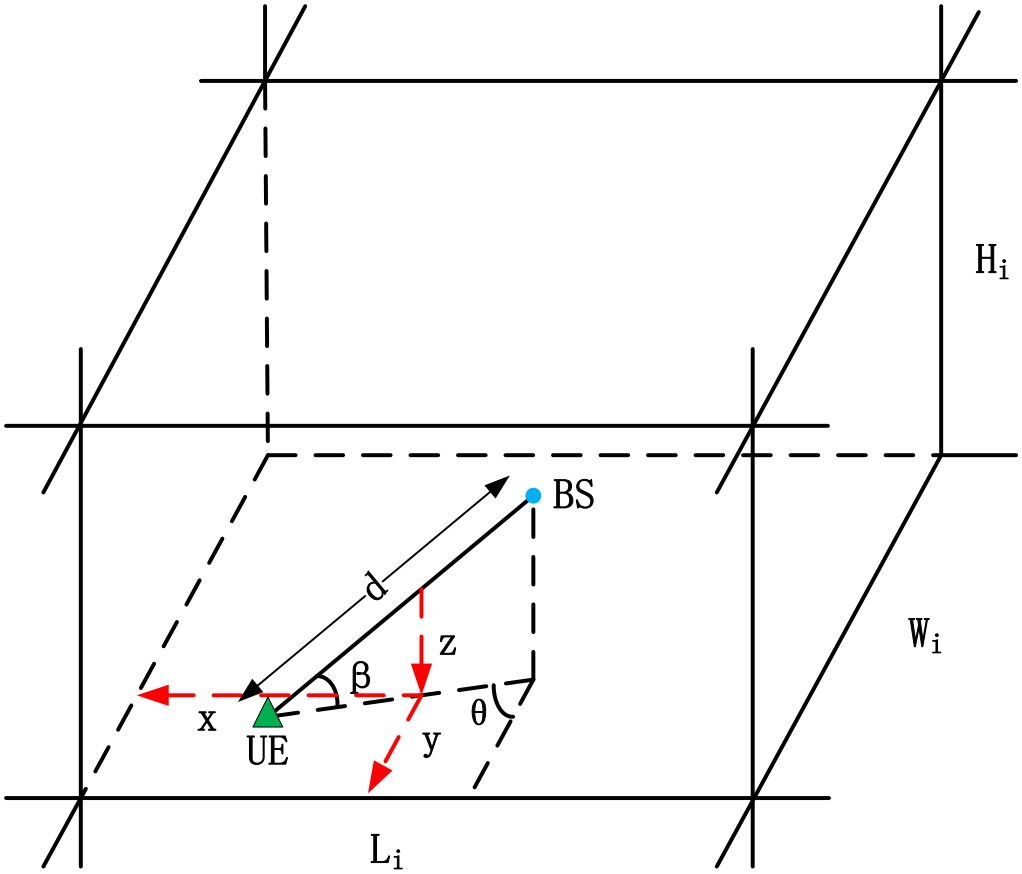

Figure 2: A simple example of a random link in single cuboid

Generally, typical indoor environments are divided into cuboids (e.g., rooms and corridors). The first step is to derive the LOS probability in a single cuboid. Then based on the result in first step, the second step is to investigate the LOS probability in the entire indoor 3D scenario. The technical procedures are presented as follows.

Step I: The LOS Probability in a Single Cuboid

This subsection will derive the LOS probability for the link between the typical user and one BS located in a single cuboid. To make the derivation clear, Fig. 2 presents a snapshot of a random propagation link in a cuboid in a 3D building grid.

The propagation link with a given distance d, whose ends are respectively the BS and the typical user, is randomly located in the 3D building grid. Both of the link's direction and middle point position are randomly generated. Assume the BS end is randomly located in a cuboid denoted by C_i with a size of L_i(length)$\times$ W_i(width)$\times$ H_i(height), as shown in Fig. 2. Without loss of generality, it is assumed that $L_i \geq W_i \geq H_i$. Thus, the

condition that this random link is LOS is that the user end is also located in the cuboid C_i. It implies that the LOS probability in the single cuboid C_i is equal to the probability that the typical user is located in the same cuboid.

Fig. 2 gives the related parameters of the random link with a length d. The acute angle between the random link and the x-y plane is denoted by β. The acute angle between the projection of the random link on the x-y plane and the y coordinate is expressed as θ. The variables x, y and z are the distances from the middle point of the random link to the nearest borders of the cuboid C_i, respectively. The variables $\beta,\ \theta,\ x,\ y$ and z are independent and distributed uniformly due to the randomness of the generated link. Their distributions are respectively denoted as

$$\begin{cases} \beta \sim U\left(0, \frac{\pi}{2}\right), \\ \theta \sim U\left(0, \frac{\pi}{2}\right), \\ x \sim U\left(0, \frac{L_i}{2}\right), \\ y \sim U\left(0, \frac{W_i}{2}\right), \\ z \sim U\left(0, \frac{H_i}{2}\right), \end{cases}$$

where U denotes the uniform distribution. Therefore, the joint probability density function $f(\beta, \theta, x, y, z)$ is given by

$$f(\theta, \beta, x, y, z) = \begin{cases} \frac{2^5}{L_i W_i H_i \pi^2}, & (\beta,\ \theta,\ x,\ y,\ z) \in\ S, \\ 0, & \text{else}, \end{cases} \tag{4}$$

where $S = \left\{\left(0 \le \beta < \frac{\pi}{2}\right) \cap \left(0 \le \theta < \frac{\pi}{2}\right) \cap \left(0 \le x < \frac{L_i}{2}\right) \cap \left(0 \le y < \frac{W_i}{2}\right) \cap \left(0 \le z < \frac{H_i}{2}\right)\right\}$.

In order to guarantee that the random link is LOS, the necessary and sufficient condition is given by

$$\left(x > \frac{d}{2}\cos\beta\sin\theta\right) \cap \left(y > \frac{d}{2}\cos\beta\cos\theta\right) \cap \left(z > \frac{d}{2}\sin\beta\right)$$

Therefore, the probability $P_{i,LOS}(d)$ that the link occurs in the cuboid C_i is LOS propagation can be derived, shown as in Theorem 1.

Theorem 1. *The LOS probability $P_{i,LOS}(d)$ in the scenario of a single cuboid with the size $L_i \times W_i \times H_i$, ($L_i \ge W_i \ge H_i$) is given by*

$$P_{i,LOS}(d) = \begin{cases} P_{i_1,LOS}(d) = \int_{B_1}\int_{\Theta_1}\int_X\int_Y\int_Z f(\theta,\beta,x,y,z)\,d\beta\,d\theta\,dx\,dy\,dz, & 0 \le d < d_{i_1} \\ P_{i_2,LOS}(d) = \int_{B_2}\int_{\Theta_2}\int_X\int_Y\int_Z f(\theta,\beta,x,y,z)\,d\beta\,d\theta\,dx\,dy\,dz, & d_{i_1} \le d < d_{i_2} \\ \quad\vdots & \\ P_{i_K,LOS}(d) = \int_{B_k}\int_{\Theta_k}\int_X\int_Y\int_Z f(\theta,\beta,x,y,z)\,d\beta\,d\theta\,dx\,dy\,dz, & d \ge d_{i_{K-1}} \end{cases} \tag{5}$$

where the LOS probability $P_{i,LOS}(d)$ is a piece-wise function determined by the link length d. Each piece is represented as $P_{i_k,LOS}(d)$, where $k = 1, 2, 3, 4, 5, 6$. B_k and Θ_k denote the integral limits of β and θ of the k-th piece, respectively. They are presented as

$$\begin{cases} B_1 \in \left(0, \frac{\pi}{2}\right), \Theta_1 \in \left(0, \frac{\pi}{2}\right); & 0 \le d < d_{i_1} \\ B_2 \in \left(0, \arcsin\frac{H_i}{d}\right), \Theta_2 \in \left(0, \frac{\pi}{2}\right); & d_{i_1} \le d < d_{i_2} \\ B_3 \in \left(0, \arcsin\frac{H_i}{d}\right), \Theta_3 \in \left(\arccos\frac{W_i}{d\cos\beta}, \frac{\pi}{2}\right); & d_{i_2} \le d < d_{i_3} \\ B_4 \in \left(0, \arcsin\frac{H_i}{d}\right), \Theta_4 \in \left(\arccos\frac{W_i}{d\cos\beta}, \arcsin\frac{L_i}{d\cos\beta}\right); & d_{i_3} \le d < d_{i_4} \\ B_5 \in \left(\arccos\frac{\sqrt{{L_i}^2+{W_i}^2}}{d}, \arcsin\frac{H_i}{d}\right), \Theta_5 \in \left(\arccos\frac{W_i}{d\cos\beta}, \arcsin\frac{L_i}{d\cos\beta}\right); & d_{i_4} \le d < d_{i_5} \\ B_6 \in \emptyset, \Theta_6 \in \emptyset; & d \ge d_{i_5} \end{cases}$$

where the values of $d_{i_1}, \ldots, d_{i_5}$ are related to the cuboid size. Specifically, $d_{i_1} = H_i$, $d_{i_2} = W_i$, $d_{i_3} = L_i$, $d_{i_4} = \sqrt{{L_i}^2 + {W_i}^2}$, and $d_{i_5} = \sqrt{{L_i}^2 + {W_i}^2 + {H_i}^2}$. X, Y and Z denote the integral limits of variables x, y and z, which are represented as $X \in \left(\frac{d}{2}\cos\beta\sin\theta, \frac{L_i}{2}\right)$, $Y \in \left(\frac{d}{2}\cos\beta\cos\theta, \frac{W_i}{2}\right)$ and $Z \in \left(\frac{d}{2}\sin\beta, \frac{H_i}{2}\right)$, respectively.

The proof of Theorem 5 is straightforwardly and is omitted here.

Theorem 1 can be generalised as the LOS probability function for any single cuboid scenario. On this basis, the LOS probability model in a 3D building scenario consisted of multiple cuboids will be obtained in the following.

Step II: The LOS Probability in a 3D Building

Generally, an indoor 3D scenario consisting of many cuboids. We assume that the entire scenario (denoted by C) is divided into N cuboids with each cuboid volume of $V_i, i = 1, 2, 3...N$. Combined with Theorem 1, the LOS probability P_{LOS} in scenario C can be obtained as in Theorem 2.

Theorem 2. *The LOS probability of a link in the indoor 3D scenario consisting of cuboids is given by*

$$P_{LOS}(d) = \sum_{i=1}^{N} \frac{V_i}{\sum_{i=1}^{N} V_i} P_{i,LOS}(d), \tag{6}$$

where $P_{i,LOS}(d)$ denotes the LOS probability function in the i-th cuboid, which has been derived in Theorem 1.

Proof. Since the BS is randomly located in the considered scenario C, the probability that the BS is located within the i-th cuboid can be presented as: $p_i = \frac{V_i}{\sum_{i=1}^{N} V_i}$. Therefore, for

the given indoor 3D scenario C, the LOS probability of a link is given by

$$P_{\mathrm{LOS}}(d) = \sum_{i=1}^{N} p_i P_{i,\mathrm{LOS}}(d), \tag{7}$$

□

Now, the LOS probability model in indoor 3D scenarios has been established. Thus, the LOS probability can be directly calculated without simulation or measurement, as long as the layout of the scenario is given. This model is analytically tractable and generally suitable to arbitrary indoor scenarios consisting of cuboids. This builds the fundamental for the performance analysis of 3D SC networks in indoor environments. Its validation will be presented in Section 4.

2.4 Performance Metrics

The main purpose of an indoor dense SC network is to improve the coverage probability for the downlink, and enhance the SE and the ASE for the overall network. Therefore, the following three performance metrics are of great importance.

1) The *coverage probability*, which is defined as the probability that the received signal to interference plus noise ratio (SINR) is larger than the threshold T :

$$p_c(\lambda_B, T) = \mathbb{P}[\mathrm{SINR} > T] \tag{8}$$

The expression of SINR will be given in the next section.

2) The *SE* in bps/Hz, which is represented as

$$\varepsilon_{SE}(\lambda_B, T_0) = \int_{T_0}^{\infty} \log_2(1+T) f_t(\lambda_B, T) \mathrm{d}T \tag{9}$$

where T_0 is the minimum required SINR value, and $f_t(\lambda_B, T)$ denotes the probability density function (PDF) of the received SINR with regard to the predefined threshold T and the BS density λ_B. Moreover, $f_t(\lambda_B, T)$ can be calculated by

$$f_t(\lambda_B, T) = \frac{\partial(1 - p_c(\lambda_B, T))}{\partial T} \tag{10}$$

3) The *ASE* in bps/Hz/km^2, which is shown as

$$\varepsilon_{ASE}(\lambda_B, T_0) = \frac{\lambda_B \cdot S \cdot B \cdot \varepsilon_{SE}}{S \cdot B} = \lambda_B \cdot \varepsilon_{SE} \tag{11}$$

where S is the area size, and B is the system bandwidth.

3 Performance Analysis

On the basis of analytical tools from stochastic geometry, this section derives the analytical and tractable expressions of the three performance metrics defined in Section 2. Firstly, the general but abstract LOS probability in equation (3) is considered, such that the corresponding results are also applicable. Then, we investigate the two-piece linear LOS probability in equation (36) as a special case in our study, following the main results obtained from the former general case. Thereafter, in the next subsection, we will use the tractable analytical results from the above special case to approximate the practical LOS probability in equation (35). The numerical results show that the approximation error is trivial.

3.1 General Case and Main Results

Without loss of generality, we assume that a typical user locates at the origin o. At first, the coverage probability is investigated according to equation (8) for the typical user, where the SINR is given by

$$\mathrm{SINR} = \frac{P_t \omega(r) h}{\sigma^2 + I_r} \tag{12}$$

where σ^2 denotes the power of the additive white Gaussian noise (AWGN), and I_r represents the total interference power from interfering BSs and is given by

$$I_r = \sum_{i:\, b_i \in \Phi_B \setminus b_0} P_t \varphi_i g_i \tag{13}$$

where b_i is the i-th interfering BS, φ_i and g_i are the path loss and power gain of Rayleigh fading between the i-th interfering BS b_i and the typical user, respectively.

Therefore, the coverage probability is obtained as follows.

Theorem 3. *For the typical user in the indoor dense SC network, considering the general LOS probability function of* $\Pr^{\mathrm{L}}(r)$ *in (3) , the coverage probability* $p_c(\lambda_B, T)$ *defined in (8) is given by*

$$p_c(\lambda_B, T) = \sum_{n=1}^{N} (C_n^L + C_n^{NL}) \tag{14}$$

where C_n^L *and* C_n^{NL} *are the n-th piece coverage probability for the situation that the typical user is connected to a BS with a LOS link and with a NLOS link, respectively.*

Moreover,

$$C_n^L = \int_{d_{n-1}}^{d_n} \mathbb{P}\left[\frac{P_t \omega_n^{\mathrm{L}}(r) h}{\sigma^2 + I_r} > T \right] f_{R,n}^{\mathrm{L}}(r) \mathrm{d}r \tag{15}$$

$$C_n^{NL} = \int_{d_{n-1}}^{d_n} \mathbb{P}\left[\frac{P_t \omega_n^{\mathrm{NL}}(r) h}{\sigma^2 + I_r} > T\right] f_{R,n}^{\mathrm{NL}}(r)\mathrm{d}r \tag{16}$$

where $f_{R,n}^{\mathrm{L}}(r)$ and $f_{R,n}^{\mathrm{NL}}(r)$ denote the n-th piece PDF of the distances R_n^{L} and R_n^{NL} from the BS to the typical user, and R_n^{L} and R_n^{NL} are the distances under the situation that the typical user is connected to a LOS BS and a NLOS BS, respectively.

Proof. According to (8) and (12), $p_c(\lambda_B, T)$ can be presented as

$$\begin{aligned}
p_c(\lambda_B, T) &= \mathbb{P}[\mathrm{SINR} > T] \\
&= \mathbb{E}_r[\mathbb{P}[\mathrm{SINR} > T|r]] \\
&= \int_{r>0} \mathbb{P}[\mathrm{SINR} > T|r] f_R(r)\mathrm{d}r \\
&= \int_{r>0} \mathbb{P}[\frac{P_t \omega(r) h}{\sigma^2 + I_r} > T] f_R(r)\mathrm{d}r \\
&\overset{(a)}{=} \int_0^{d_1} \mathbb{P}[\frac{P_t \omega_1^{\mathrm{L}}(r) h}{\sigma^2 + I_r} > T] f_{R,1}^{\mathrm{L}}(r)\mathrm{d}r + \int_0^{d_1} \mathbb{P}[\frac{P_t \omega_1^{\mathrm{NL}}(r) h}{\sigma^2 + I_r} > T] f_{R,1}^{\mathrm{NL}}(r)\mathrm{d}r \\
&\quad + \cdots \\
&\quad + \int_{d_{N-1}}^{\infty} \mathbb{P}[\frac{P_t \omega_N^{\mathrm{L}}(r) h}{\sigma^2 + I_r} > T] f_{R,N}^{\mathrm{L}}(r)\mathrm{d}r + \int_{d_{N-1}}^{\infty} \mathbb{P}[\frac{P_t \omega_N^{\mathrm{NL}}(r) h}{\sigma^2 + I_r} > T] f_{R,N}^{\mathrm{NL}}(r)\mathrm{d}r \\
&= \sum_{n=1}^{N} (C_n^L + C_n^{NL})
\end{aligned} \tag{17}$$

where step (a) follows from the definition of $f_R(r)$, which is the PDF of the distance between the typical user and its serving BS, given by

$$f_R(r) = \begin{cases}
f_{R,1}(r) = \begin{cases} f_{R,1}^{\mathrm{L}}(r), & \text{with LOS connection} \\ f_{R,1}^{\mathrm{NL}}(r), & \text{with NLOS connection} \end{cases}, & 0 \le r \le d_1 \\
f_{R,2}(r) = \begin{cases} f_{R,2}^{\mathrm{L}}(r), & \text{with LOS connection} \\ f_{R,2}^{\mathrm{NL}}(r), & \text{with NLOS connection} \end{cases}, & d_1 < r \le d_2 \\
\vdots & \vdots \\
f_{R,N}(r) = \begin{cases} f_{R,N}^{\mathrm{L}}(r), & \text{with LOS connection} \\ f_{R,N}^{\mathrm{NL}}(r), & \text{with NLOS connection} \end{cases}, & r > d_{N-1}
\end{cases} \tag{18}$$

Obviously, $f_R(r)$ has a similar formalization as (1). Besides, we have $f_{R,n}(r) = f_{R,n}^{\mathrm{L}}(r) + f_{R,n}^{\mathrm{NL}}(r)$, because the two conditions that the typical user is connected to a LOS BS or a NLOS BS are disjoint events. □

As can be seen from Theorem 3, if we want to derive the coverage probability, the key point is to obtain functions $f_{R,n}^{\mathrm{L}}(r)$, $f_{R,n}^{\mathrm{NL}}(r)$, and the probability $\mathbb{P}\left[\frac{P_t\omega_n^{\mathrm{L}}(r)h}{\sigma^2+I_r} > T\right]$, $\mathbb{P}\left[\frac{P_t\omega_n^{\mathrm{NL}}(r)h}{\sigma^2+I_r} > T\right]$.

Hence, the results of them are presented in Lemma 4 and Lemma 5, respectively.

Lemma 4. *In Theorem 3, considering the smallest-path-loss user association strategy,* $f_{R,n}^{\mathrm{L}}(r)$ *and* $f_{R,n}^{\mathrm{NL}}(r)$ *are given by*

$$\begin{aligned} f_{R,n}^{\mathrm{L}}(r) = 2\pi r\lambda_B \times \mathrm{Pr}_n^{\mathrm{L}}(r) \times \exp\left(-2\pi\lambda_B \int_0^r \mathrm{Pr}^{\mathrm{L}}(t)t\mathrm{d}t\right) \\ \times \exp\left(-2\pi\lambda_B \int_0^{r_1} \left(1-\mathrm{Pr}^{\mathrm{L}}(t)\right) t\mathrm{d}t\right) \end{aligned} \tag{19}$$

and

$$\begin{aligned} f_{R,n}^{\mathrm{NL}}(r) = 2\pi r\lambda_B \times \left(1-\mathrm{Pr}_n^{\mathrm{L}}(r)\right) \times \exp\left(-2\pi\lambda_B \int_0^{r} \left(1-\mathrm{Pr}^{\mathrm{L}}(t)\right) t\mathrm{d}t\right) \\ \times \exp\left(-2\pi\lambda_B \int_0^{r_2} \mathrm{Pr}^{\mathrm{L}}(t)t\mathrm{d}t\right) \end{aligned} \tag{20}$$

respectively, where the variables r_1 *and* r_2 *can be calculated by,*

$$r_1 = \arg_{r_1}\left\{\omega^{NL}(r_1) = \omega_n^L(r)\right\} \tag{21}$$

and

$$r_2 = \arg_{r_2}\left\{\omega^{L}(r_2) = \omega_n^{NL}(r)\right\} \tag{22}$$

Proof. Firstly, we derive $f_{R,n}^{\mathrm{L}}(r)$ as follows.

As mentioned before, $f_{R,n}^{\mathrm{L}}(r)$ is the n-th piece PDF of the distance R_n^{L}, under the situation that the typical user is connected to the serving BS with a LOS path. Thus, under the smallest-path-loss UAS, the following two conditions should be satisfied,

1) Condition A1 : For the typical user, the serving BS is with a shortest LOS path.

2) Condition A2 : For the typical user, the serving BS goes through a smaller path loss than the nearest BS with a NLOS path.

In order to formulate the above two conditions, the distance between the typical user and the nearest BS with a LOS path is denoted as X^{L}. Then, for condition A1, no other BSs with the LOS paths can be closer than X^{L}. So,the complementary cumulative distribution function (CCDF) of X^{L} is formulated as

$$F_{X^{\mathrm{L}}}(x) = 1 - \exp\left(-\lambda_B \int_0^x \mathrm{Pr}^{\mathrm{L}}(t)2\pi t\mathrm{d}t\right) \tag{23}$$

Therefore, the PDF of X^{L} can be found as

$$\begin{aligned} f_{X^{\mathrm{L}}}(x) &= \frac{\partial F_{X^{\mathrm{L}}}(x)}{\partial x} \\ &= 2\pi x \lambda_B \mathrm{Pr}^{\mathrm{L}}(x) \times \exp\left(-\lambda_B \int_0^x \mathrm{Pr}^{\mathrm{L}}(t) 2\pi t \mathrm{d}t\right) \end{aligned} \tag{24}$$

For condition A2, there should be no NLOS BS for the user within a circle with a radius $x_1 < x$, which has the smaller path loss than the nearest LOS BS at the distance $X^{\mathrm{L}} = x$. Moreover, $x_1 = \arg_{x_1}\left\{\omega^{NL}(x_1) = \omega_n^L(x)\right\}$. So, the conditional probability of A2 can be derived as

$$\mathbb{P}[\mathrm{A2}|X^{\mathrm{L}} = x] = \exp\left(-\lambda_B \int_0^{x1} \left(1 - \mathrm{Pr}^{\mathrm{L}}(t)\right) 2\pi t \mathrm{d}t\right) \tag{25}$$

The next step calculates the PDF of R^{L}, which is the distance from the user to its designated BS. At first step, the distribution of R^{L} is given by

$$\begin{aligned} F_{R^{\mathrm{L}}}(r) &= \mathbb{E}_{X^{\mathrm{L}}}\left\{\mathbb{P}[R^{\mathrm{L}} > r|X^{\mathrm{L}}]\right\} \\ &= \int_0^{\infty} \mathbb{P}[R^{\mathrm{L}} > r|X^{\mathrm{L}} = x] f_{X^{\mathrm{L}}}(x) \mathrm{d}x \\ &\overset{(a)}{=} \int_0^{r} 0 \times f_{X^{\mathrm{L}}}(x) \mathrm{d}x + \int_r^{\infty} \mathbb{P}[A2|X^{\mathrm{L}} = x] f_{X^{\mathrm{L}}}(x) \mathrm{d}x \\ &= \int_r^{\infty} \mathbb{P}[A2|X^{\mathrm{L}} = x] f_{X^{\mathrm{L}}}(x) \mathrm{d}x \end{aligned} \tag{26}$$

where the step (a) follows the fact that when $0 < x \leq r$, then $\mathbb{P}[R^{\mathrm{L}} > r|X^{\mathrm{L}} = x] = 0$; and when $x > r$, then $\mathbb{P}[R^{\mathrm{L}} > r|X^{\mathrm{L}} = x] = \mathbb{P}[A2|X^{\mathrm{L}} = x]$.

Therefore, the PDF of R^{L} is formulated as

$$f_{R^{\mathrm{L}}}(r) = \mathbb{P}[A2|X^{\mathrm{L}} = r] f_{X^{\mathrm{L}}}(r) \tag{27}$$

For the n-th piece $d_{n-1} < x \leq d_n$, we can have

$$\begin{aligned} f_{R,n}^{\mathrm{L}}(r) = 2\pi r \lambda_B \times \mathrm{Pr}_n^{\mathrm{L}}(r) \times \exp\left(-2\pi\lambda_B \int_0^r \mathrm{Pr}^{\mathrm{L}}(t) t \mathrm{d}t\right) \\ \times \exp\left(-2\pi\lambda_B \int_0^{r_1} \left(1 - \mathrm{Pr}^{\mathrm{L}}(t)\right) t \mathrm{d}t\right) \end{aligned} \tag{28}$$

Similarly, $f_{R,n}^{\mathrm{NL}}(r)$ can also be derived, and the derivation is omitted here. □

Lemma 5. *In Theorem 3,* $\mathbb{P}\left[\frac{P_t \omega_n^{\mathrm{L}}(r) h}{\sigma^2 + I_r} > T\right]$ *and* $\mathbb{P}\left[\frac{P_t \omega_n^{\mathrm{NL}}(r) h}{\sigma^2 + I_r} > T\right]$ *are given by*

$$\mathbb{P}\left[\frac{P_t \omega_n^{\mathrm{L}}(r) h}{\sigma^2 + I_r} > T\right] = \exp\left(-\frac{T\sigma^2}{P_t \omega_n^{\mathrm{L}}(r)}\right) \times \mathcal{L}_{I_r}^{\mathrm{L}}\left(\frac{T}{P_t \omega_n^{\mathrm{L}}(r)}\right) \tag{29}$$

and

$$\mathbb{P}\left[\frac{P_t\omega_n^{\mathrm{NL}}(r)h}{\sigma^2+I_r}>T\right]=\exp\left(-\frac{T\sigma^2}{P_t\omega_n^{\mathrm{NL}}(r)}\right)\times\mathcal{L}_{I_r}^{\mathrm{NL}}\left(\frac{T}{P_t\omega_n^{\mathrm{NL}}(r)}\right) \tag{30}$$

respectively. Herein, $\mathcal{L}_{I_r}^{\mathrm{L}}(s)$ and $\mathcal{L}_{I_r}^{\mathrm{NL}}$ denote the Laplace transform of I_r for the LOS and NLOS propagation, respectively. They can be computed by the following equations,

$$\begin{aligned}\mathcal{L}_{I_r}^{\mathrm{L}}(s)=&\exp\left(-2\pi\lambda_B\int_r^{\infty}\frac{\mathrm{Pr}^{\mathrm{L}}(t)t}{1+(sP_t\omega^{\mathrm{L}}(t))^{-1}}\mathrm{d}t\right)\\&\times\exp\left(-2\pi\lambda_B\int_{r1}^{\infty}\frac{[1-\mathrm{Pr}^{\mathrm{L}}(t)]t}{1+(sP_t\omega^{\mathrm{NL}}(t))^{-1}}\mathrm{d}t\right)\end{aligned} \tag{31}$$

$$\begin{aligned}\mathcal{L}_{I_r}^{\mathrm{NL}}(s)=&\exp\left(-2\pi\lambda_B\int_{r_2}^{\infty}\frac{\mathrm{Pr}^{\mathrm{L}}(t)t}{1+(sP_t\omega^{\mathrm{L}}(t))^{-1}}\mathrm{d}t\right)\\&\times\exp\left(-2\pi\lambda_B\int_{r}^{\infty}\frac{[1-\mathrm{Pr}^{\mathrm{L}}(t)]t}{1+(sP_t\omega^{\mathrm{NL}}(t))^{-1}}\mathrm{d}t\right)\end{aligned} \tag{32}$$

Proof.

$$\begin{aligned}\mathbb{P}\left[\frac{P_t\omega_n^{\mathrm{L}}(r)h}{\sigma^2+I_r}>T\right]&=\mathbb{E}_{I_r}\left\{\mathbb{P}\left[h>\frac{T(\sigma^2+I_r)}{P_t\omega_n^{\mathrm{L}}(r)}\right]\right\}\\&\overset{(a)}{=}\mathbb{E}_{I_r}\left\{\exp\left(-\frac{T(\sigma^2+I_r)}{P_t\omega_n^{\mathrm{L}}(r)}\right)\right\}\\&=\exp\left(-\frac{T\sigma^2}{P_t\omega_n^{\mathrm{L}}(r)}\right)\mathbb{E}_{I_r}\left\{\exp\left(-\frac{TI_r}{P_t\omega_n^{\mathrm{L}}(r)}\right)\right\}\\&=\exp\left(-\frac{T\sigma^2}{P_t\omega_n^{\mathrm{L}}(r)}\right)\mathcal{L}_{I_r}^{\mathrm{L}}\left(\frac{T}{P_t\omega_n^{\mathrm{L}}(r)}\right)\end{aligned} \tag{33}$$

where step (a) is obtained based on the distribution of fading h, i.e., $h\sim\exp(1)$.

In addition, based on the smallest-path-loss user association strategy, $\mathcal{L}_{I_r}^{\mathrm{L}}(s)$ is derived as

$$\begin{aligned}\mathcal{L}_{I_r}^{\mathrm{L}}(s)&=\mathbb{E}_{I_r}\left\{\exp(-sI_r)|\text{ LOS connection for the typical user}\right\}\\&=\mathbb{E}_{[\Phi_B,\varphi_i,g_i]}\left\{\exp\left(-s\sum_{i:\,b_i\in\Phi_B\setminus b_0}P_t\varphi_ig_i\right)\right\}\\&\overset{(b)}{=}\exp\left(-2\pi\lambda_B\int_r^{\infty}\mathrm{Pr}^{\mathrm{L}}(t)\times\left[1-\mathbb{E}_g[\exp(-sP_t\omega^{\mathrm{L}}(t)g)]\right]t\mathrm{d}t\right)\\&\quad\times\exp\left(-2\pi\lambda_B\int_{r_1}^{\infty}\left[1-\mathrm{Pr}^{\mathrm{L}}(t)\right]\times\left[1-\mathbb{E}_g[\exp(-sP_t\omega^{\mathrm{NL}}(t)g)]\right]t\mathrm{d}t\right)\\&\overset{(c)}{=}\exp\left(-2\pi\lambda_B\int_r^{\infty}\frac{\mathrm{Pr}^{\mathrm{L}}(t)t}{1+(sP_t\omega^{\mathrm{L}}(t))^{-1}}\mathrm{d}t\right)\\&\quad\times\exp\left(-2\pi\lambda_B\int_{r1}^{\infty}\frac{[1-\mathrm{Pr}^{\mathrm{L}}(t)]t}{1+(sP_t\omega^{\mathrm{NL}}(t))^{-1}}\mathrm{d}t\right)\end{aligned} \tag{34}$$

where step (b) is obtained from the PGFL. Step (c) is calculated from $g \sim \exp(1)$.

Note that the former exponential function represents the aggregate interference from the LOS paths, and the latter represents the aggregate interference from the NLOS paths.

Similarly, $\mathbb{P}\left[\frac{P_t \omega_n^{\mathrm{NL}}(r) h}{\sigma^2 + I_r} > T\right]$ and $\mathcal{L}_{I_r}^{\mathrm{NL}}(s)$ can also be derived. The proof of them is omitted here. □

From Theorem 3, Lemma 4 and Lemma 5, it is observed that the coverage probability $p_c(\lambda_B, T)$ is determined by the following three important functions: piece-wise LOS and NLOS path loss function $\omega_N^{\mathrm{L}}(r)$ and $\omega_N^{\mathrm{NL}}(r)$, as well as the piece-wise LOS probability function $\mathrm{Pr}_n^{\mathrm{L}}(r)$. Therefore, the next section will numerically evaluate their impacts on the indoor dense SC network.

Corollary 6. *For computing the SE, the simple step is to substitute (14) into (10), and then get the result using (9). Similarly, for computing the ASE, we can substitute the result obtained from (9) into (11).*

Note that, the SE and the ASE are affected differently by the density of BSs, which will be shown in the next section as well.

3.2 Special Case and Main Results

In this subsection, the performance analysis of indoor SC networks will be investigated with the special case of an indoor 2D SC network. Firstly, the LOS probability for the indoor 2D SC network, which is a special case of the proposed LOS probability model for indoor 3D SC network, is applied. Secondly, on the basis of the general results we have obtained in the previous subsection, the performance metrics for this special case will be derived.

A. The approximation of LOS probability model

On the basis of the proposed 3D LOS probability model in Section 2, the LOS probability model for indoor 2D scenarios can be obtained. Combined with the works [11] and [13], the exact LOS probability model for a 2D typical indoor environment is obtained as

follows

$$\Pr^{\mathrm{L}}(r)=\begin{cases}\frac{4}{5D^2\pi}\left[r^2-4rD+D^2\right]+\frac{1}{5LM\pi}\left[r^2-2r(L+M)+LM\pi\right], & 0<r\le d_1\\ \frac{4}{5D^2\pi}\left[-L^2+2rM(\sqrt{1-\frac{L^2}{r^2}}-1)+2LM\arcsin\frac{L}{r}\right] & \\ +\left[r^2-4rD+D^2\right]+\frac{1}{5LM\pi}, & d_1<r\le d_2\\ \frac{4}{5D^2\pi}\left[-D^2+2rD(\sqrt{1-\frac{D^2}{r^2}}-1)+2D^2\arcsin\frac{D}{r}\right] & \\ +\frac{1}{5LM\pi}\left[-L^2+2rM(\sqrt{1-\frac{L^2}{r^2}}-1)+2LM\arcsin\frac{L}{r}\right], & d_2<r\le d_3\\ \frac{1}{5LM\pi}\left[-L^2+2rM(\sqrt{1-\frac{L^2}{r^2}}-1)+2LM\arcsin\frac{L}{r}\right], & d_3<r\le d_4\\ \frac{1}{5LM\pi}\Big[r^2+L^2+M^2-2r(M\sqrt{1-\frac{L^2}{r^2}}+L\sqrt{1-\frac{M^2}{r^2}}) & \\ +2LM(\arccos\frac{L}{r}+\arccos\frac{M}{r}-2\pi)\Big]\frac{-1}{LM\pi}, & d_4<r\le d_5\\ 0, & r>d_5\end{cases}\tag{35}$$

where the parameters d_1 to d_5 are link distances, and the parameters $D, L,$ and M present the layout of the considered scenario. The details can be found in [11] and [13].

In order to derive the tractable expression of the performance metrics, we use some elementary functions (e.g., linear functions) to approximate the LOS probability model, since its expression is sophisticated. For tractability, a two-piece approximation function is adopted [9], which is given by

$$\Pr^{\mathrm{L}}(r)=\begin{cases}1-\frac{r}{L_1}, & 0<r\le L_1\\ 0, & r>L_1\end{cases}\tag{36}$$

where L_1 is an important parameter which can be explained as the LOS possibility of a given transmission environment. In other words, the larger L_1 is, the less obstacles the propagating environment contains, and then the higher the LOS probability is at a provided link distance. Moreover, L_1 can be adjusted to match the complicated LOS probability function, which will be shown in Section 4.

As previously mentioned, in this subsection, the two-piece linear LOS probability function shown as in (36) is applied as a special case of Theorem 3. That is explained as follows: (1) using the linear LOS probability function can lead to more tractable analytical results for the system model with LOS and NLOS transmission; (2) using the linear LOS probability function can easily approximate the practical but complex LOS probability function, e.g. (35).

Owing to the current cellular frequency band that is lower than 6GHz, the path loss exponent α^{L} for LOS path is assumed to be the same for all segments of the path loss model. The same assumption also applies to α^{NL}.

According to Theorem 3, the coverage probability (8) is given by

$$p_c(\lambda_B, T) = \sum_{n=1}^{2} (C_n^L + C_n^{NL}) \tag{37}$$

where C_1^L, C_1^{NL}, C_2^L and C_2^{NL} are derived in the following parts.

B. The derivation of C_1^L

Based on (15) and (29), C_1^L can be computed by

$$\begin{aligned} C_1^L &= \int_0^{L_1} \mathbb{P}\left[\frac{P_t \omega_1^{\mathrm{L}}(r) h}{\sigma^2 + I_r} > T\right] f_{R,1}^{\mathrm{L}}(r)\mathrm{d}r \\ &= \int_0^{L_1} \exp\left(-\frac{T\sigma^2}{P_t \omega_1^{\mathrm{L}}(r)}\right) \times \mathcal{L}_{I_r}^{\mathrm{L}}\left(\frac{T}{P_t \omega_1^{\mathrm{L}}(r)}\right) f_{R,1}^{\mathrm{L}}(r)\mathrm{d}r \\ &= \int_0^{L_1} \exp\left(-\frac{T\sigma^2 r^{\alpha^{\mathrm{L}}}}{P_t K^{\mathrm{L}}}\right) \times \mathcal{L}_{I_r}^{\mathrm{L}}\left(\frac{T r^{\alpha^{\mathrm{L}}}}{P_t K^{\mathrm{L}}}\right) f_{R,1}^{\mathrm{L}}(r)\mathrm{d}r \end{aligned} \tag{38}$$

Intuitively, in order to compute C_1^L, the expressions of $f_{R,1}^{\mathrm{L}}(r)$ and $\mathcal{L}_{I_r}^{\mathrm{L}}(s)$ should be obtained firstly. From Lemma 4 and (19), we have

$$\begin{aligned} f_{R,1}^{\mathrm{L}}(r) &= 2\pi r \lambda_B \times (1 - \frac{r}{L_1}) \times \exp\left(-2\pi\lambda_B \int_0^r (1 - \frac{t}{L_1}) t \mathrm{d}t\right) \\ &\quad \times \exp\left(-2\pi\lambda_B \int_0^{r_1} \frac{t}{L_1} t \mathrm{d}t\right) \\ &= 2\pi r \lambda_B \times (1 - \frac{r}{L_1}) \times \exp\left(-\pi\lambda_B r^2 + \frac{2\pi\lambda_B}{3L_1}(r^3 - r_1^3)\right) \end{aligned} \tag{39}$$

when $0 < r \leq L_1$. Moreover, according to (21), the variable r_1 is given by

$$r_1 = \left(\frac{K^{\mathrm{NL}}}{K^{\mathrm{L}}}\right)^{\frac{1}{\alpha^{\mathrm{NL}}}} r^{\frac{\alpha^{\mathrm{L}}}{\alpha^{\mathrm{NL}}}} \tag{40}$$

According to Lemma 5 and (31), the Laplace transform of the aggregate interference for the LOS transmission is represented as

$$\begin{aligned} \mathcal{L}_{I_r}^{\mathrm{L}}(s) &= \exp\left(-2\pi\lambda_B \int_r^{L_1} \left(1 - \frac{t}{L_1}\right) \times \frac{t}{1 + (sP_t K^{\mathrm{L}} t^{-\alpha^{\mathrm{L}}})^{-1}} \mathrm{d}t\right) \\ &\quad \times \exp\left(-2\pi\lambda_B \int_{r_1}^{L_1} \left(\frac{t}{L_1}\right) \times \frac{t}{1 + (sP_t K^{\mathrm{NL}} t^{-\alpha^{\mathrm{NL}}})^{-1}} \mathrm{d}t\right) \\ &\quad \times \exp\left(-2\pi\lambda_B \int_{L_1}^{\infty} 1 \times \frac{t}{1 + (sP_t K^{\mathrm{NL}} t^{-\alpha^{\mathrm{NL}}})^{-1}} \mathrm{d}t\right) \end{aligned} \tag{41}$$

Note that, due to $0 < r \leq L_1$, the aggregate interference comes from both LOS and NLOS paths. On the right-hand side of equation (41), the first item denotes the aggregate interference from LOS paths, while the second and third items are the aggregate interference from NLOS paths.

Finally, substituting (39) and (41) into (38), the detailed expression of C_1^L can be obtained.

C. The derivation of C_1^{NL}

Based on (16) and (30), C_1^{NL} is computed by

$$\begin{aligned} C_1^{NL} &= \int_0^{L_1} \mathbb{P}\left[\frac{P_t\omega_1^{\mathrm{NL}}(r)h}{\sigma^2+I_r} > T\right] f_{R,1}^{\mathrm{NL}}(r)\mathrm{d}r \\ &= \int_0^{L_1} \exp\left(-\frac{T\sigma^2}{P_t\omega_1^{\mathrm{NL}}(r)}\right) \times \mathcal{L}_{I_r}^{\mathrm{NL}}\left(\frac{T}{P_t\omega_1^{\mathrm{NL}}(r)}\right) f_{R,1}^{\mathrm{NL}}(r)\mathrm{d}r \\ &= \int_0^{L_1} \exp\left(-\frac{T\sigma^2 r^{\alpha^{\mathrm{NL}}}}{P_tK^{\mathrm{NL}}}\right) \times \mathcal{L}_{I_r}^{\mathrm{NL}}\left(\frac{Tr^{\alpha^{\mathrm{NL}}}}{P_tK^{\mathrm{NL}}}\right) f_{R,1}^{\mathrm{NL}}(r)\mathrm{d}r \end{aligned} \tag{42}$$

Intuitively, in order to compute C_1^{NL}, the expressions of $f_{R,1}^{\mathrm{NL}}(r)$ and $\mathcal{L}_{I_r}^{\mathrm{NL}}(s)$ should be obtained first. From Lemma 4 and (20),

$$\begin{aligned} f_{R,1}^{\mathrm{NL}}(r) = 2\pi r\lambda_B \times (\frac{r}{L_1}) \times \exp\left(-2\pi\lambda_B \int_0^r (\frac{t}{L_1})t\mathrm{d}t\right) \\ \times \exp\left(-2\pi\lambda_B \int_0^{r_2} (1-\frac{t}{L_1})t\mathrm{d}t\right), \end{aligned} \tag{43}$$

for $0 < r \leq L_1$. Moreover, according to (22), the variable r_2 is given by

$$r_2 = \left(\frac{K^{\mathrm{L}}}{K^{\mathrm{NL}}}\right)^{\frac{1}{\alpha^{\mathrm{L}}}} r^{\frac{\alpha^{\mathrm{NL}}}{\alpha^{\mathrm{L}}}} \tag{44}$$

Note that, different from the case (only one condition $r_1 < L_1$) for computing $f_{R,1}^{\mathrm{L}}(r)$, there are two conditions for computing $f_{R,1}^{\mathrm{NL}}(r)$: $r_2 > L_1$ and $r_2 \leq L_1$.

Condition (1): When $0 < r_2 \leq L_1$, namely, $0 < r \leq u_1 = L_1^{\frac{\alpha^{\mathrm{L}}}{\alpha^{\mathrm{NL}}}} \left(\frac{K^{\mathrm{NL}}}{K^{\mathrm{L}}}\right)^{\frac{1}{\alpha^{\mathrm{L}}}}$, the expression of $f_{R,1}^{\mathrm{NL}}(r)$ is derived as

$$\begin{aligned} f_{R,1}^{\mathrm{NL}}(r) &= 2\pi r\lambda_B \times (\frac{r}{L_1}) \times \exp\left(-2\pi\lambda_B \int_0^r (\frac{t}{L_1})t\mathrm{d}t\right) \\ &\quad \times \exp\left(-2\pi\lambda_B \int_0^{r_2} (1-\frac{t}{L_1})t\mathrm{d}t\right) \\ &= 2\pi r\lambda_B \times (\frac{r}{L_1}) \times \exp\left(-\pi\lambda_B r_2^2 + \frac{2\pi\lambda_B}{3L_1}(r_2^3 - r^3)\right), \end{aligned} \tag{45}$$

when $0 < r \leq u_1$.

Condition (2): When $r_2 > L_1$, namely, the expression of $u_1 < r \leq L_1$, $f_{R,1}^{\mathrm{NL}}(r)$ is

$$\begin{aligned} f_{R,1}^{\mathrm{NL}}(r) &= 2\pi r\lambda_B \times (\frac{r}{L_1}) \times \exp\left(-2\pi\lambda_B \int_0^r (\frac{t}{L_1}) t \mathrm{d}t\right) \\ &\quad \times \exp\left(-2\pi\lambda_B \int_0^{L_1} (1 - \frac{t}{L_1}) t \mathrm{d}t\right) \\ &= 2\pi r\lambda_B \times (\frac{r}{L_1}) \times \exp\left(-\pi\lambda_B \left(\frac{L_1^2}{3} + \frac{2r^3}{3L_1}\right)\right) \end{aligned} \tag{46}$$

when $u_1 < r \leq L_1$.

Accordingly, there are two different expressions of the aggregate interference corresponding to the above two conditions.

Condition (1): when $0 < r \leq u_1$, according to Lemma 5 and equation (32), the Laplace transform of the aggregate interference for the NLOS transmission is expressed as

$$\begin{aligned} \mathcal{L}_{I_r}^{\mathrm{NL}}(s) &= \exp\left(-2\pi\lambda_B \int_{r_2}^{L_1} \left(1 - \frac{t}{L_1}\right) \times \frac{t}{1 + (sP_tK^{\mathrm{L}}t^{-\alpha^{\mathrm{L}}})^{-1}} \mathrm{d}t\right) \\ &\quad \times \exp\left(-2\pi\lambda_B \int_{r}^{L_1} \left(\frac{t}{L_1}\right) \times \frac{t}{1 + (sP_tK^{\mathrm{NL}}t^{-\alpha^{\mathrm{NL}}})^{-1}} \mathrm{d}t\right) \\ &\quad \times \exp\left(-2\pi\lambda_B \int_{L_1}^{\infty} 1 \times \frac{t}{1 + (sP_tK^{\mathrm{NL}}t^{-\alpha^{\mathrm{NL}}})^{-1}} \mathrm{d}t\right) \end{aligned} \tag{47}$$

when $0 < r \leq u_1$.

Condition (2): when $u_1 < r \leq L_1$, according to Lemma 5 and equation (32), the Laplace transform of the aggregate interference for the NLOS transmission is represented as

$$\begin{aligned} \mathcal{L}_{I_r}^{\mathrm{NL}}(s) &= \exp\left(-2\pi\lambda_B \int_{r}^{L_1} \left(\frac{t}{L_1}\right) \times \frac{t}{1 + (sP_tK^{\mathrm{NL}}t^{-\alpha^{\mathrm{NL}}})^{-1}} \mathrm{d}t\right) \\ &\quad \times \exp\left(-2\pi\lambda_B \int_{L_1}^{\infty} 1 \times \frac{t}{1 + (sP_tK^{\mathrm{NL}}t^{-\alpha^{\mathrm{NL}}})^{-1}} \mathrm{d}t\right) \end{aligned} \tag{48}$$

when $u_1 < r \leq L_1$.

Note that, the aggregate interference in condition (1) comes from both LOS and NLOS paths. However, the aggregate interference in condition (2) comes from NLOS paths only.

Finally, C_1^{NL} is computed as

$$\begin{aligned} C_1^{NL} &= \int_0^{u_1} \exp\left(-\frac{T\sigma^2 r^{\alpha^{\mathrm{NL}}}}{P_tK^{\mathrm{NL}}}\right) \times \left(\mathcal{L}_{I_r}^{\mathrm{NL}}\left(\frac{Tr^{\alpha^{\mathrm{NL}}}}{P_tK^{\mathrm{NL}}}\right) f_{R,1}^{\mathrm{NL}}(r) \middle| 0 < r \leq u_1\right) \mathrm{d}r \\ &\quad + \int_{u_1}^{L_1} \exp\left(-\frac{T\sigma^2 r^{\alpha^{\mathrm{NL}}}}{P_tK^{\mathrm{NL}}}\right) \times \left(\mathcal{L}_{I_r}^{\mathrm{NL}}\left(\frac{Tr^{\alpha^{\mathrm{NL}}}}{P_tK^{\mathrm{NL}}}\right) f_{R,1}^{\mathrm{NL}}(r) \middle| u_1 < r \leq L_1\right) \mathrm{d}r \end{aligned} \tag{49}$$

where (45), (46), (47) and (48) are substituted into (49).

D. The derivation of C_2^L

Based on (15) and (29), C_2^L can be obtained by

$$\begin{aligned} C_2^L &= \int_{L_1}^{\infty} \mathbb{P}\left[\frac{P_t\omega_2^{\mathrm{L}}(r)h}{\sigma^2+I_r} > T\right] f_{R,2}^{\mathrm{L}}(r)\mathrm{d}r \\ &= \int_{L_1}^{\infty} \exp\left(-\frac{T\sigma^2}{P_t\omega_2^{\mathrm{L}}(r)}\right) \times \mathcal{L}_{I_r}^{\mathrm{L}}\left(\frac{T}{P_t\omega_2^{\mathrm{L}}(r)}\right) f_{R,2}^{\mathrm{L}}(r)\mathrm{d}r \\ &= \int_{L_1}^{\infty} \exp\left(-\frac{T\sigma^2 r^{\alpha^{\mathrm{L}}}}{P_tK^{\mathrm{L}}}\right) \times \mathcal{L}_{I_r}^{\mathrm{L}}\left(\frac{Tr^{\alpha^{\mathrm{L}}}}{P_tK^{\mathrm{L}}}\right) f_{R,2}^{\mathrm{L}}(r)\mathrm{d}r \end{aligned} \tag{50}$$

Intuitively, in order to compute C_2^L, the expressions of $f_{R,2}^{\mathrm{L}}(r)$ and $\mathcal{L}_{I_r}^{\mathrm{L}}(s)$ should be obtained first. From Lemma 4 and equation (19), we have

$$\begin{aligned} f_{R,1}^{\mathrm{L}}(r) &= 2\pi r\lambda_B \times 0 \times \exp\left(-2\pi\lambda_B \int_0^r \Pr^{\mathrm{L}}(t)t\mathrm{d}t\right) \\ &\quad \times \exp\left(-2\pi\lambda_B \int_0^{r_1} \left(1-\Pr^{\mathrm{L}}(t)\right)t\mathrm{d}t\right) \\ &= 0 \end{aligned} \tag{51}$$

Therefore, we have $C_2^L = 0$.

E. The derivation of C_2^{NL}

Based on (16) and (30), C_2^{NL} can be computed by

$$\begin{aligned} C_2^{NL} &= \int_{L_1}^{\infty} \mathbb{P}\left[\frac{P_t\omega_2^{\mathrm{NL}}(r)h}{\sigma^2+I_r} > T\right] f_{R,2}^{\mathrm{NL}}(r)\mathrm{d}r \\ &= \int_{L_1}^{\infty} \exp\left(-\frac{T\sigma^2}{P_t\omega_2^{\mathrm{NL}}(r)}\right) \times \mathcal{L}_{I_r}^{\mathrm{NL}}\left(\frac{T}{P_t\omega_2^{\mathrm{NL}}(r)}\right) f_{R,2}^{\mathrm{NL}}(r)\mathrm{d}r \\ &= \int_{L_1}^{\infty} \exp\left(-\frac{T\sigma^2 r^{\alpha^{\mathrm{NL}}}}{P_tK^{\mathrm{NL}}}\right) \times \mathcal{L}_{I_r}^{\mathrm{NL}}\left(\frac{Tr^{\alpha^{\mathrm{NL}}}}{P_tK^{\mathrm{NL}}}\right) f_{R,2}^{\mathrm{NL}}(r)\mathrm{d}r \end{aligned} \tag{52}$$

The functions of $f_{R,2}^{\mathrm{NL}}(r)$ and $\mathcal{L}_{I_r}^{\mathrm{NL}}(s)$ are calculated first. From Lemma 4 and equation (20), we have

$$\begin{aligned} f_{R,2}^{\mathrm{NL}}(r) &= 2\pi r\lambda_B \times \exp\left(-2\pi\lambda_B\left(\int_0^{L_1}(\frac{t}{L_1})t\mathrm{d}t + \int_{L_1}^{r} t\mathrm{d}t\right)\right) \\ &\quad \times \exp\left(-2\pi\lambda_B \int_0^{L_1}(1-\frac{t}{L_1})t\mathrm{d}t\right) \\ &= \exp(-\pi\lambda_B r^2)2\pi\lambda_B r \end{aligned} \tag{53}$$

when $r > L_1$.

Through Lemma 5 and equation (32), the Laplace transform of the aggregate interference for NLOS transmissions is calculated as

$$\mathcal{L}_{I_r}^{\mathrm{NL}}(s) = \exp\left(-2\pi\lambda_B \int_r^{\infty} 1 \times \frac{t}{1+(sP_tK^{\mathrm{NL}}t^{-\alpha^{\mathrm{NL}}})^{-1}}\mathrm{d}t\right) \tag{54}$$

when $r > L_1$.

Here, the aggregate interference only comes from NLOS paths.

Finally, substituting (53) and (54) into (52), the detailed expression of C_2^{NL} can be obtained.

F. The derivation of three performance metrics

Based on equation (37) and the results from Subsections A-E, the coverage probability is obtained as follows

$$p_c(\lambda_B, T) = C_1^L + C_1^{NL} + C_2^{NL} \tag{55}$$

where C_1^L, C_1^{NL} and C_2^{NL} are shown as (38), (49) and (52), respectively.

In the same way, according to Corollary 6, the tractable expressions of the SE and the ASE will be calculated through substituting the function of $p_c(\lambda_B, T)$ into equations (7) and (9), respectively.

4 Numerical Results and Discussion

This section numerically evaluates the analytical results of the proposed LOS probability model in 3D scenarios in Section 2 and the performance metrics obtained in Section 3. Firstly, the proposed LOS probability in 3D scenarios shown as in Theorem 1 is validated by comparing to Monte Carlo simulation. Secondly, the approximated results of the LOS probability equation (35) by the linear equation (36) for an indoor 2D scenario are presented. The validation of the approximation method is shown through numerical results and Monte Carlo simulations. Then, the impact of different LOS functions on network performance metrics is illustrated. Moreover, the differences of the network performance are demonstrated based on two types of path loss model: the simplistic path loss model with single slope and the practical piece-wise path loss model with LOS or NLOS transmissions.

Unless otherwise stated, the following parameters are set for the channel model: $\alpha_1^{\mathrm{L}} = \alpha_2^{\mathrm{L}} = 1.69, \alpha_1^{\mathrm{NL}} = \alpha_2^{\mathrm{NL}} = 4.33, K_1^{\mathrm{L}} = K_2^{\mathrm{L}} = 10^{-3.28}, K_1^{\mathrm{NL}} = K_2^{\mathrm{NL}} = 10^{-1.15}, P_t = 24dBm, \sigma^2 = -95dBm$, in accordance with the indoor SC channel of 3GPP standard [12].

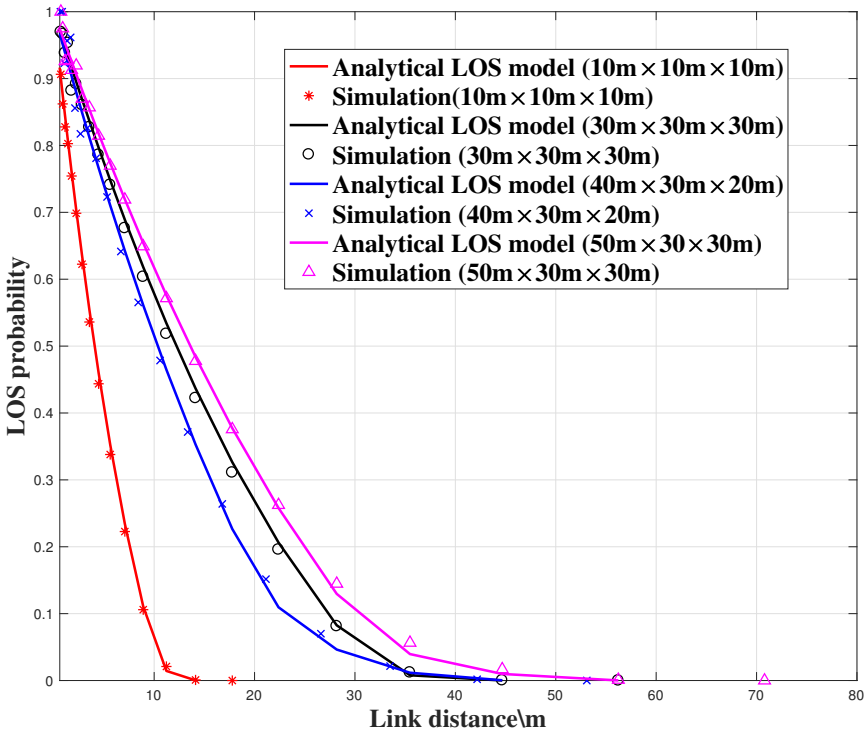

Figure 3: Validation of the proposed 3D LOS probability model

A. Validation of the proposed 3D LOS probability model

The proposed LOS probability for indoor 3D scenarios as shown in Theorem 1 is validated in this subsection. The analytical results obtained from Theorem 1 are compared to Monte Carlo simulations with various cuboid sizes: $10m \times 10m \times 10m$, $30m \times 30m \times 30m$, $40m \times 30m \times 20m$, and $50m \times 30m \times 30m$. Observing from Fig. 3, the analytical results fit the simulation results closely. Moreover, the LOS probability keeps reducing with the increase of link distance, and also is influenced by the cuboid size.

B. Validation of the approximated LOS probability functions

This subsection evaluates the practical LOS probability function (35) for the performance analysis in the indoor SC network. Its related parameters are based on the work [13]. In order to match this practical model well by using approximated method, L_1 is set to $8.4m$ so that (36) can intersect with (35) at the point with LOS probability 0.5. The results are shown in Fig. 4. In addition, the approximated LOS probability functions with other different parameters of $L_1 = 48.4m$ and $L_1 = 88.4m$ are also shown in Fig. 4, which

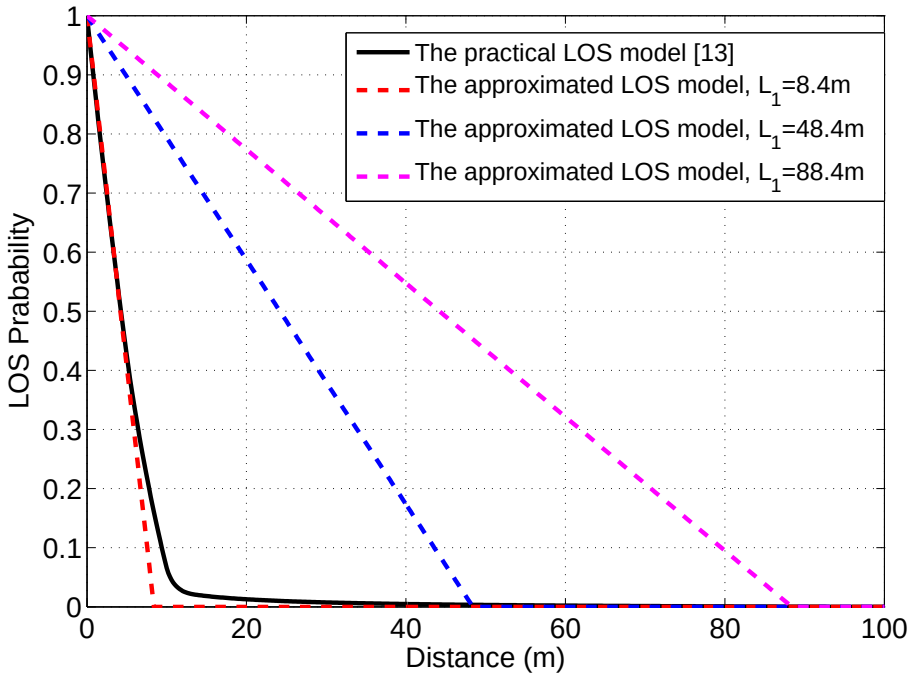

Figure 4: The practical LOS probability functions and the approximated LOS probability functions

are chosen randomly and only for the subsequent researches, e.g. the influence of various propagation environments on the indoor dense SC networks.

In order to demonstrate the validation of the approximated LOS probability model, we present the comparison between the Monte Carlo simulations of coverage probability based on (35) and the numerical results of coverage probability based on (36) with $L_1 = 8.4m$. The results are shown in Fig. 5. It is observed that the analytical results present a good match for the simulation results when the density of BS is large. In terms of the relatively small BS density, only very small gaps exist, which is caused by the approximation of the LOS probability, but its effects are trivial. Therefore, we will directly use numerical results of the approximated LOS model to analyse the indoor network performance later.

C. Discussion about three performance metrics

In this Subsection, we discuss the relationship between the BS density and the three critical performance metrics defined in Section 2. Moreover, the effects of the different propagation environments, i.e., different LOS probability functions, on the network performance are also uncovered. In order to highlight the characteristics of the indoor dense SC network with LOS and NLOS transmissions, the traditional single-slope path loss model

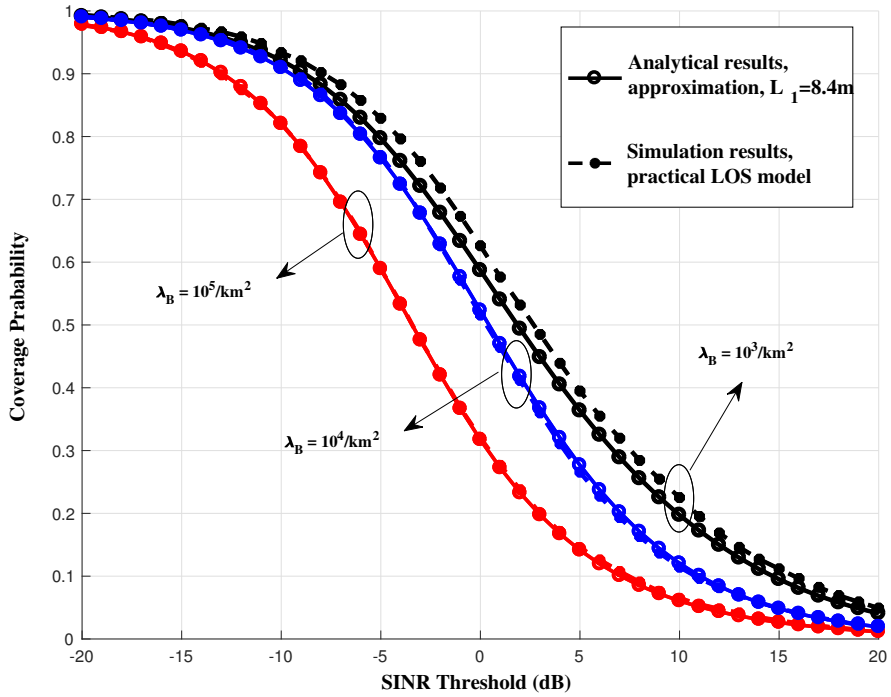

Figure 5: The coverage probability vs. the SINR threshold

is adopted [4]. Following the reference, its path loss exponent is set as $\alpha = \alpha^{\mathrm{NL}} = 4.33$.

In Fig. 6, it's clearly seen that significant differences exist between the coverage probability analysis using our proposed model and the analysis in [4]. In [4], the coverage probability increases with the BS density λ_B first since the distance is shorter between the user and the designated BS. Then, the coverage probability keeps constant and becomes independent of λ_B, when the BS density λ_B becomes sufficiently large. This is because although more inter-cell interference is introduced by the dense SC network, the increase in interference power is counterbalanced by the increase in received desired signal power. However, for the analysis through the proposed model with $L_1 = 8.4m$ by distinguishing between LOS and NLOS transmissions, the coverage probability increases at first, and then decreases after reaching the peak value when λ_B is around $10^3 BSs/km^2$. The reason for this trend is that with the denser deployment of BSs, the more NLOS transmissions between the interfering BSs and the typical users are transformed into LOS transmissions due to the closer transmission distances.

Meantime, Fig. 6 demonstrates that the coverage probability performance is also affected by the LOS probability functions. It's clear that the peak value of the coverage probability becomes more sharp and moves towards left, with the parameter L_1 increasing

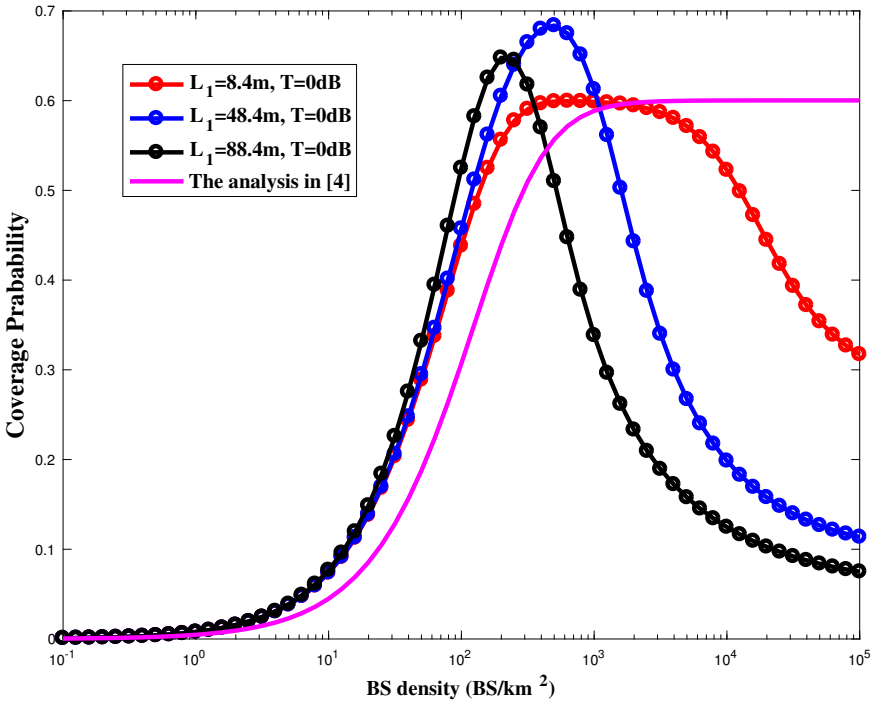

Figure 6: The coverage probability vs. the BS density (the threshold of SINR T = 0dB)

(from 8.4m to 48.4m to 88.4m). This indicates that the optimal density of BSs for maximizing the coverage probability is related to the parameter L_1, which decreases with the increase of L_1. It's reasonable because the propagation environment becomes sparser with the larger L_1, which leads to the faster transformation from NLOS to LOS.

In order to demonstrate the generality of the above conclusions, we also give the coverage probability performance analysis with the SINR threshold different from the Fig. 6. The observations obtained from Fig. 7 are similar to Fig. 6, although their values of the SINR threshold are different.

Fig. 8 shows the SE versus the BS density, which is similar to the trend of curves in Fig. 6. This is because the SE is mainly decided by the coverage probability according to the equation (9).

Fig. 9 demonstrates the ASE performance versus the BS density. Compared with the SE, the ASE performance is more dependent on the BS density. Based on the analysis in [4], the ASE increases linearly with λ_B when the BSs are enough dense. It's reasonable because the coverage probability is constant and is independent of λ_B under such ultra-dense transmission environments. However, in the network performance analysis with our proposed model, the ASE increases super-linearly with λ_B for low-density indoor networks,

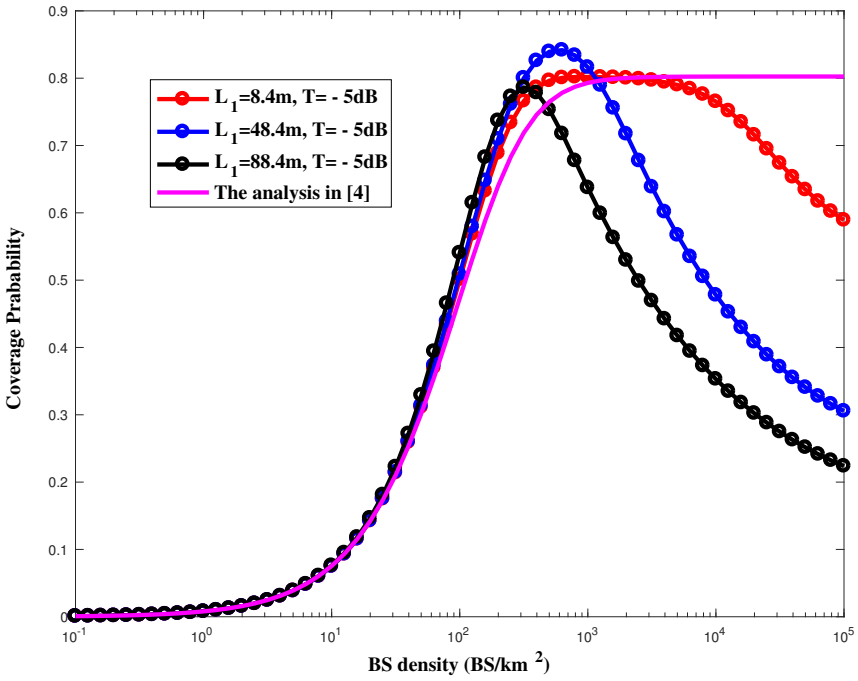

Figure 7: The coverage probability vs. the BS density (the threshold of SINR: T = -5dB)

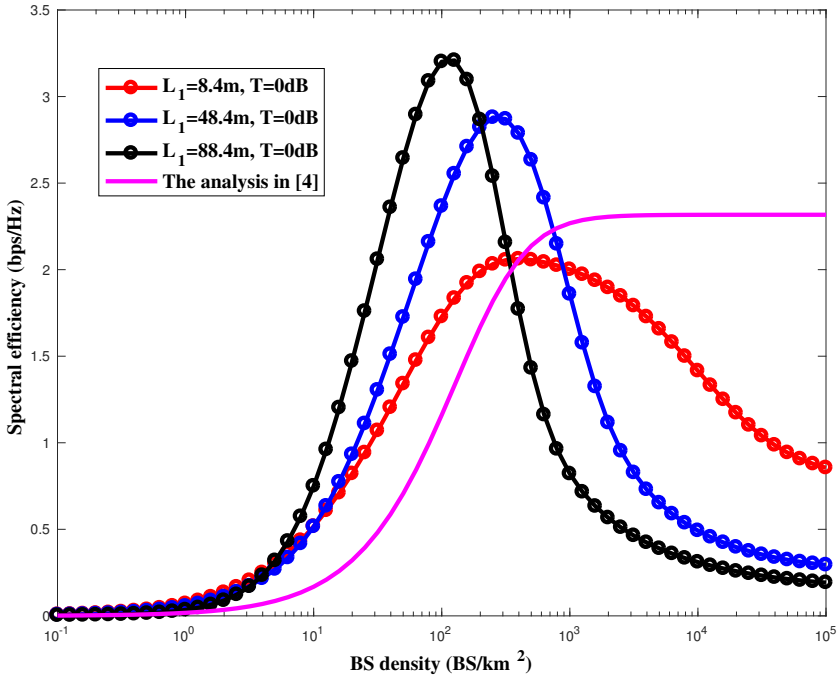

Figure 8: The SE vs. the BS density (the threshold of SINR: T = 0dB)

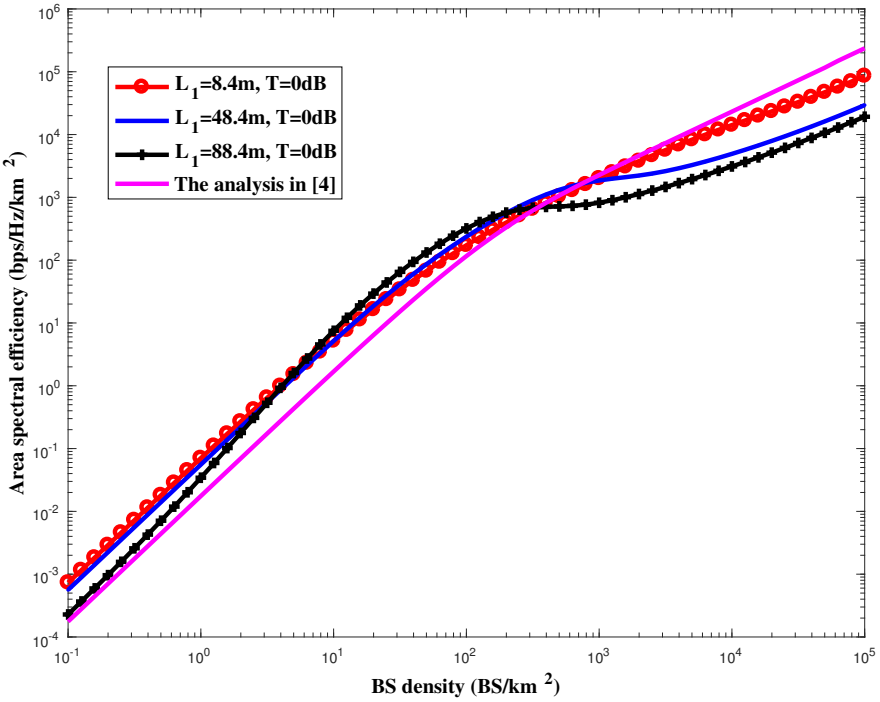

Figure 9: The ASE vs. the BS density (the threshold of SINR: T = 0dB)

but increases sub-linearly with λ_B for high-density indoor networks. The reason is that the ASE is affected by both the SE and the densification of BSs.

5 Conclusion

This deliverable has developed a tractable path loss model by distinguishing between LOS and NLOS transmission from LOS and NLOS path and has proposed a novel LOS probability function in indoor 3D scenarios. The path loss model and the LOS probability function are then utilized to analyse the performance limits of indoor 3D SC networks. On the basis of stochastic geometry, three performance metrics, including coverage probability, SE and ASE, are derived analytically with a practical path loss model and a special path loss model, respectively. The analytical results are validated by comparing with Monte Carlo simulations. Simulation results reveal that the performance metrics aforementioned are affected by the BS density and the link LOS probability. Specifically, the different influence of LOS and NLOS propagations is notable. As a consequence, the results obtained in this deliverable provide an approach to investigate the performance limits of the indoor dense SC networks in 3D scenarios. For future work, on the basis of

the proposed approach, the performance analysis of dense SC networks with 3D MIMO will be fully investigated.

References

[1] J. G. Andrews, S. Buzzi, W. Choi, S. V. Hanly, A. Lozano, A. C. Soong, and J. C. Zhang, "What will 5G be?" *IEEE J. Sel. Areas Commun.*, vol. 32, no. 6, pp. 1065–1082, Jun. 2014.

[2] M. Kamel, H. Hamouda, and A. Youssef, "Ultra-dense networks: A survey," *IEEE Commun. Surveys Tuts.*, vol. 18, no. 4, pp. 2522–2545, May 2016.

[3] L. Zhang, X. Yu, Z. Liu, L. Zhang, and H. Moon, "Modeling and analysis of indoor coverage probability for future 3D dense mobile networks," in *Proc. 20th Int. Symp. Wireless Pers. Multimedia Commun. (WPMC)*, Dec. 2017, pp. 247–252.

[4] J. G. Andrews, F. Baccelli, and R. K. Ganti, "A tractable approach to coverage and rate in cellular networks," *IEEE Trans. Commun.*, vol. 59, no. 11, pp. 3122–3134, Nov. 2011.

[5] H. S. Dhillon, R. K. Ganti, F. Baccelli, and J. G. Andrews, "Modeling and analysis of K-tier downlink heterogeneous cellular networks," *IEEE J. Sel. Areas Commun.*, vol. 30, no. 3, pp. 550–560, Apr. 2012.

[6] S. Singh, H. S. Dhillon, and J. G. Andrews, "Offloading in heterogeneous networks: Modeling, analysis, and design insights," *IEEE Trans. Wireless Commun.*, vol. 12, no. 5, pp. 2484–2497, May 2013.

[7] X. Zhang and J. G. Andrews, "Downlink cellular network analysis with multi-slope path loss models," *IEEE Trans. Commun.*, vol. 63, no. 5, pp. 1881–1894, Mar. 2015.

[8] C. Galiotto, N. K. Pratas, N. Marchetti, and L. Doyle, "A stochastic geometry framework for LOS/NLOS propagation in dense small cell networks," in *Proc. IEEE Int. Conf. on Commun. (ICC)*, 2015, pp. 2851–2856.

[9] M. Ding, P. Wang, D. López-Pérez, G. Mao, and Z. Lin, "Performance impact of LoS and NLoS transmissions in dense cellular networks," *IEEE Trans. on Wireless Commun.*, vol. 15, no. 3, pp. 2365–2380, Mar. 2016.

[10] T. Ding, M. Ding, G. Mao, Z. Lin, D. López-Pérez, and A. Y. Zomaya, "Uplink performance analysis of dense cellular networks with LoS and NLoS transmissions," *IEEE Trans. on Wireless Commun.*, vol. 16, no. 4, pp. 2601–2613, Apr. 2017.

[11] H. Zheng, "Performance analysis of indoor wireless communications in dense cellular networks," *Ph.D. thesis, the University of Sheffield, Sheffield, UK*, 2018.

[12] 3GPP, "TR 36.873 (V12.7.0): Study on 3D channel model for LTE," 2017.

[13] H. Zheng, J. Zhang, H. Hu, H. Li, Q. Hong, and J. Zhang, "Exact Line-of-Sight probability for channel modelling in typical indoor environments," *IEEE Antennas Wireless Propag. Lett.*, vol. 17, pp. 1359 –1362, Jul. 2018.